ADVANCED FUNCTIONAL MATERIALS
www.afm-journal.de

Bio-Inspired Synthesis of Minerals for Energy, Environment, and Medicinal Applications

*Sungjin Kim and Chan Beum Park**

Biomineralization, the natural pathway of assembling biogenic inorganic compounds, inspires us to exploit unique, effective strategies to fabricate functional materials with intricate structures. In this article, the recent advances in bio-inspired synthesis of minerals—with a focus on those of calcium-based minerals—and their applications to the design of functional materials for energy, environment, and biomedical fields are reviewed. Biomimetic mineralization is extending its application range to unconventional area such as the design of component materials for lithium-ion batteries and elaborately structured composite materials utilizing carbon dioxide gas. Materials with highly enhanced mechanical properties are synthesized through emulating the nacre structure. Studies of bioactive minerals-carbon hybrid materials show an expansion of potential applications to fields ranging from interdisciplinary science to practical engineering such as the fabrication of reinforced bone-implantable materials.

1. Introduction

Biomineralization is a natural pathway of producing intricately structured inorganic materials that possess vital functions in biologic systems. The highly ordered architectures and diverse morphologies of biominerals motivated scientists to mimic these materials through the study of the underlying chemistry of biomineralization.[1–3] In fact, the synthesis of materials that resemble complex morphologies of natural biominerals is one of key fields in biomimetic science.[1–12] Furthermore, the pursuit of mimicking natural biomineralization while comprehending its mechanism has enabled the replication of the outstanding mechanical and optical properties of biominerals with their unique biologic functions, such as navigation, storage, and homeostasis.[1,4,13–15] Calcium-based biominerals, such as calcium carbonates ($CaCO_3$) and hydroxyapatites [$Ca_{10}(PO_4)_6(OH)_2$], have been popularly studied to emulate their crucial structural and biologic functions as shells and bones,[1] respectively, as well as to artificially control their protean morphologies and properties in their crystallization process in vitro.[9–11] For example, the fabrication of materials that mimic the unique structure and strength of bone[16] or exhibit bone-forming bioactivity is a highly demanded task in materials science as well as in biomedical fields.[17] Indeed, it has been an interest since prehistoric times, when attempts to replace missing teeth were made by using shells, corals, ivories, and bones from dead humans or animals,[18] which were the primitive form of biomimetic applications for orthopedic treatment, bone regeneration and tissue engineering.[19–23]

The current pursuit of biomimetic mineralization goes beyond the fabrication of mimetic materials to nature's sophisticated structures or their biologic functions. Increasing studies have been reporting the results implying good possibilities that bio-inspired mineralization or its derivatives can become virtuous implements to synthesize functional materials in fields ranging from energy to medicine, regardless of whether they originally contained the specific context of biomimetic mineralization. Therefore, it is needed to newly evaluate the recent progresses and future prospects in the extensive application scope of bio-inspired/biomimetic mineralization, as briefly illustrated in **Scheme 1**. This review primarily, but not exclusively, covers the applications of $CaCO_3$ and hydroxyapatites for their importance in the studies of bio-inspired systems as well as for their abundance in nature as the representatives of skeletal/exoskeletal components of miscellaneous organisms.[1] We concentrate on the unconventional applications such as bio-inspired fabrication of energy materials for lithium ion batteries and CO_2 mineralization for synthesizing highly ordered functional materials (**Table 1**). We also discuss the assembly of nacre-mimetic hybrid structures with enhanced mechanical properties and the synthesis of hybrid materials of bioactive minerals with carbon nanomaterials (e.g., carbon nanotube, graphene). In the later part of this article, we briefly summarize recent issues in biomedical applications including the syntheses of bone-bioactive materials and carriers for drug delivery systems.

S. Kim,[+] Prof. C. B. Park
Department of Materials Science and Engineering
Korea Advanced Institute of Science
and Technology (KAIST)
335 Science Road, Daejeon 305-701
Republic of Korea
Website: http://biomaterials.kaist.ac.kr
E-mail: parkcb@kaist.ac.kr
[+] Current address: Advanced Technology R&D Center, SKC Co., Ltd., Suwon 440-301, Republic of Korea

DOI: 10.1002/adfm.201201994

2. Bio-Inspired Mineralization for Energy and Environmental Applications

2.1. Synthesis of Component Materials for Li-Ion Batteries

Global energy issues, such as the depletion of fossil fuels in the near future, are continuously escalating along with environmental challenges including accumulation of CO_2 and global warming. Rechargeable Li-ion batteries are considered as a candidate for sustainable and clean route to energy storage. In this respect, many studies have been carried out on designing component materials (e.g., cathode/anode active materials, battery separator and electrolyte) for Li-ion batteries.[24,25] Recent studies suggest that bio-inspired mineralization can be a powerful approach to fabricate component materials for Li-ion batteries that exhibit high performance in terms of power, charge/discharge properties, and capacity retention.

2.1.1. Synthesis of Electrode Materials

Electrode active materials are typically composed of inorganic oxide compounds. For example, lithium transition metal oxides such as lithium cobalt oxide (LCO, $LiCoO_2$), lithium manganese oxide (LMO, $LiMn_2O_4$) and lithium iron phosphate (LFP, $LiFePO_4$) are applied as common active materials for cathodes, while lithiniated graphite (LiC_6) is widely applied for anodes in commercial Li-ion batteries.[26] Belcher et al.[27–30] recently applied biomimetic mineralization of viruses to the unique, effective fabrication of both cathode and anode active materials for Li-ion batteries. They utilized genetically engineered M13 viruses coated with peptide groups that have a high affinity for single-walled carbon nanotubes (SWNTs) and peptides capable of nucleating amorphous $FePO_4$ (a-$FePO_4$) for fabricating cathodes in high-power Li-ion batteries.[27,28] This virus-templated a-$FePO_4$/SWNT hybrid showed specific capacity value comparable to up-to-date commercial crystalline $LiFePO_4$. It also showed stable capacity retention during 50 cycles, indicating structural stability induced by the material-specific binding and robust framework of CNTs. This bio-inspired method of nanowiring highly conductive CNTs with electrode active materials enables environmentally benign, low-temperature fabrication of high-performance electrodes even from materials with low electronic conductivity. Anode materials were also synthesized by means of a similar process.[29,30] They produced stamped microbattery electrodes with full electrochemical functionality by the self-assembly of virus-templated cobalt oxide (Co_3O_4) nanowires.[29] It served as an anode material on top of micro-scale islands of polyelectrolytes multilayers comprising cationic linear-polyethylenimine (LPEI) and anionic polyacrylic acid (PAA) on polydimethylsiloxane (PDMS) stamp (**Figure 1**). Such microbattery electrodes could be easily stamped on various rigid or flexible substrates to design microbatteries of inter-digitated or 3D architecture with stable, reliable performance. According to another study,[30] anode material could also be formed using gold and silver noble metals and their alloy nanowires via the analogous M13 virus toolkit. In the study, pure Au, Ag, and their alloys with diameters below 50 nm were successfully synthesized as a template for the fabrication of an anode material using two clones of M13 virus, which were respectively genetically engineered for specificity and versatility. Such bio-inspired synthesis of an anode material through the mineralization of viruses enabled easy control over particle sizes, morphologies, and compositions. It also exhibited electrochemical activity towards Li even in bulk powder form as well as in the form of thin film.

A combination of biomimetic mineralization and peptide self-assembly was recently used for the fabrication of cathode materials. The self-assembly of peptide-based building blocks is considered to be an effective way to synthesize functional materials because of functional flexibility and environmental compatibility.[31,32] For example, diphenylalanine (Phe-Phe, FF) and its derivatives are simplest peptides that show extraordinary mechanical,[33] electrochemical,[34] and optical properties,[35] as well as high thermal and chemical stabilities.[36] Besides, they can self-assemble into eclectic nanostructures such as nanotubes,[33–35,37] nanowires,[35,38] nanospheres,[39] organogels,[40] and hydrogels.[41] Ryu et al.[42] succeeded in the synthesis of peptide/transition metal phosphate core/shell nanofibers using a peptide self-assembly (**Figure 2**). The nanofibers were initially prepared by the self-assembly of fluorenylmethoxycarbonyl FF peptides. Their acidic and polar moieties facilitated the mineralization

Sungjin Kim received his BS and MS degrees in materials science and engineering from KAIST, under the supervision of Professor Chan Beum Park. He also studied at the same department of Georgia Institute of Technology as an undergraduate exchange student. He is currently an associate research engineer in SKC Co., Ltd., a subsidiary of SK Group. His research interests include biomimetic mineralization, organic–inorganic hybrid materials, and Li-ion battery separators.

Chan Beum Park is an associate professor at the department of Materials Science and Engineering, KAIST. Currently, he serves as a director of National Research Laboratory supported by the Korean Government. He received BS, MS, and PhD degrees in chemical engineering from POSTECH, and worked as a post-doctoral researcher at the University of California, Berkeley, USA. His research group focuses on the development of bio-inspired functional materials for applications in energy and healthcare.

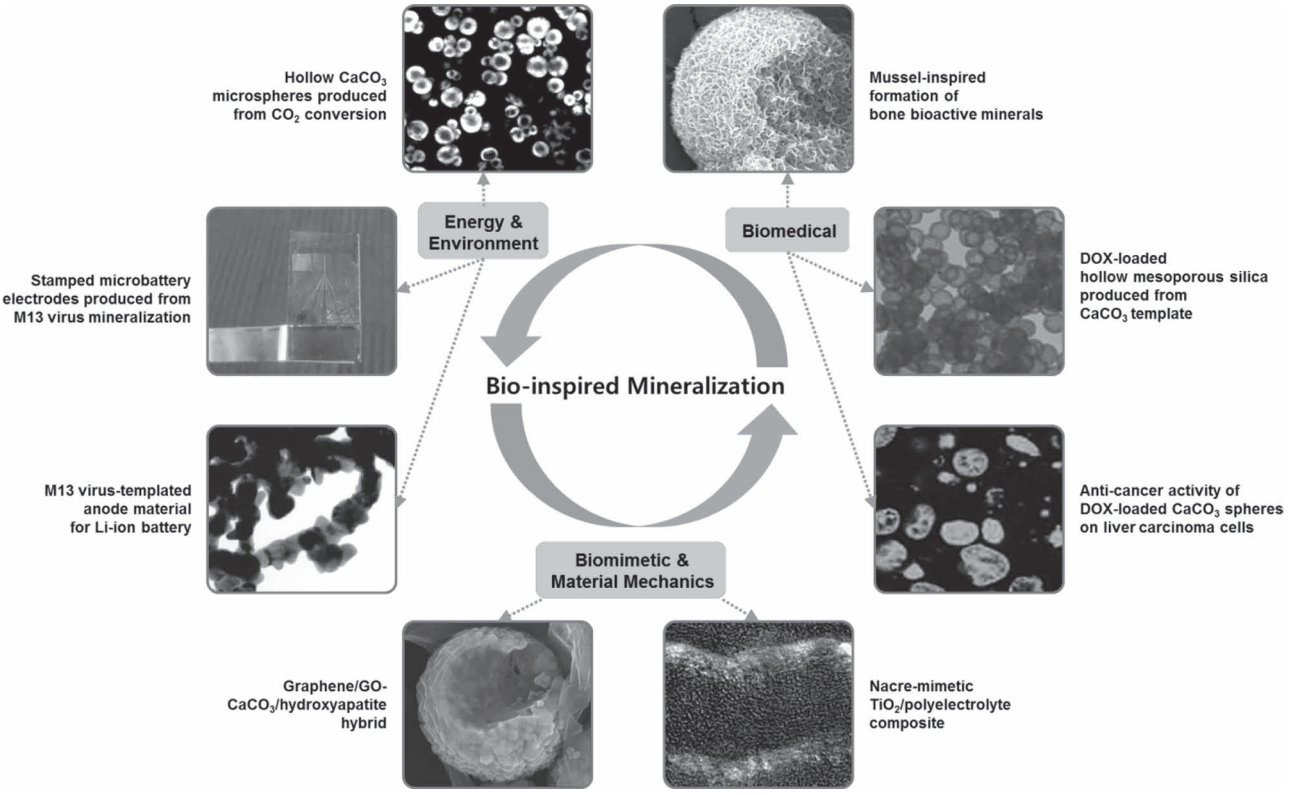

Scheme 1. Potential application fields for bio-inspired mineralization, ranging from energy to healthcare. Reproduced with permission.[29] Copyright 2008, National Academy of Sciences; ref. [30], Copyright 2010, American Chemical Society; ref. [58], Copyright 2011, Royal Society of Chemistry; ref. [80], Copyright 2009, American Chemical Society; ref. [101]; ref. [126], Copyright 2010, Elsevier Limited; ref. [144], Copyright 2008, American Chemical Society.

of $FePO_4$ on the surface of peptide nanofibers. Subsequently, $FePO_4$ nanotubes with inner walls that were coated with a conductive carbon layer were created by the carbonization of the peptide core at 350 °C. The core/shell structure showed a highly reversible capacity and good capacity retention during cycling.

On the other hand, Imai et al. synthesized manganese oxide (MnO_2) nanostructures for cathode materials by a microbial-inspired mineralization of transition metal oxide.[43] Both enzyme-mediated and abiotic oxidation processes involve biomineralization of manganese and iron oxides in microbial mineralization.[44,45] Bacteria can produce transition metal oxides with controlled nanostructures and oxidation states in an aqueous solution. The combination of organic molecules, comprising antioxidants and chelating agents, played an important role in the parallel control of oxidation states and morphologies at room temperature, which synthetically imitates such biogenic processes. A stable, divalent $Mn(OH)_2$ powder could be selectively obtained by using ascorbic acid as an antioxidizing agent and other organic molecules (e.g. polyacrylic acid, citric acid) to chelate Mn^{2+} ions. Subsequently, $Mn(OH)_2$ underwent the topotactic oxidation to selectively form trivalent manganese oxyhydroxide (β-MnOOH) (**Figure 3**A) and trivalent/tetravalent sodium manganese oxide (birnessite, $Na_{0.55}Mn_2O_4 \cdot 1.5H_2O$). Thus-formed β-MnOOH showed a good performance with improved stability within 60 cycles of charge-discharge as a cathode material for Li-ion batteries (Figure 3B). Their another study shows that a highly porous, spinel-type $LiMn_2O_4$ framework with 3D architectures could be successfully produced by a biomimetic solution route.[46] A nanoscopically ordered architecture of $MnCO_3$ nanocrystals that resembles hierarchical structure of biological $CaCO_3$ calcite was formed in an organic gel (agar) matrix. The spinel-type $LiMn_2O_4$ was produced from thus-formed $MnCO_3$ architecture through Mn_2O_3 as an intermediate phase. The pore volume in the rhombohedral body could be controllably increased by increasing the agar gel concentration, isolating the $MnCO_3$ nanocrystal units. The cycle performance of highly porous sample produced from the highest agar concentration (i.e., 4.0 wt%) showed maintenance of the highest specific capacity and the most stable cycle performance throughout the 20 cycles at high current density. Its highly porous structure for effective electrochemical reaction as well as 3D-structured channels for good ionic diffusion resulted in a high durability in Li^+ ion insertion/extraction process at a high current density. It further led to a high rate of capability and durability as a cathode for Li-ion batteries.

2.1.2. Synthesis of Battery Separator

The battery separator is a physical barrier between cathode and anode, which prevents electrical short-circuits while permitting ionic flow between the electrodes. It is a microporous membrane, usually made of polyolefins, that plays an important

Table 1. Examples of bio-inspired mineralization for the synthesis of functional materials that possess elaborate structures.

Application fields	Applications	Examples	References
Energy and environment	Li-ion batteries	Virus-templated cathode materials	[27,28]
		Virus-templated anode materials	[29,30]
		Peptide-templated cathode materials	[42]
		Microbial mineralization-inspired cathode materials	[43]
		Calcite-mimetic spinel type cathode materials	[46]
		$CaCO_3$-composite separators	[48]
	CO_2 utilization	Hollow $CaCO_3$ microspheres	[58]
		Hydroxyapatite-polycaprolactone composite scaffolds	
		Vaterite spheroids	[71]
		$CaCO_3$-biopolymer thin-films	[72,73]
		Nacre-mimetic structure	[74]
		Collagen-mimetic structure	[75]
Material mechanics (Biomimetic)	Nacre-mimetic structures	Silica-PDDMA composites	[78]
		$CaCO_3$-PAA-chitosan composites	[81]
		$CaCO_3$-PAA-diazo composite	[74]
		K_2SO_4-PAA composite	[82]
		Freeze-casting processed composites	[79,83,84]
		(e.g. porous and layered hybrids of organic-inorganic composites	
		brick-and-mortal composite structures of Al_2O_3 and PMMA)	
		TiO_2-polyelectrolyte composites	[80]
(Interdisciplinary)	CNT-biomineral hybrids	CNT-hydroxyapatite coating on Ti-6Al-4V substrate	[88–92]
		(by laser alloying, plasma spraying process),	
		Polydopamine-induced CNT-hydroxyapatite composites	[93]
	Graphene-biomineral hybrids	GO/graphene-vaterite hybrid films	[101]
		GO/graphene-incorporated hydroxyapatite films	
Biomedical	Bone bioactive materials	Bioactive glasses	[120–122]
		Polydopamine coated substrates	[123]
		Dopamine-induced $CaCO_3$ vaterite	[125]
		Dopamine-induced carbonated hydroxyapatite	[126]
	Drug delivery system	Protein (e.g. BSA, hydrophobin, BMP-2) carriers	[115–118,129,135–137]
		Anti-inflammatory drug (e.g., vancomycin, ibuprofen, captopril) carriers	[132,138,139]
		Drug delivery monitoring via photoluminescence	[140,141]
		(hydroxyapatite - xeolite composite)	
		Anti-cancer drug (e.g. Pt complexes, DOX) carriers	[131,139,142–146]

role in the safety and stability of batteries.[24,47] It is currently more required for a separator to endure mechanical damage or high temperature to prevent its rupture or melt-down causing electrical short-circuit at high voltage or at high charge/discharge rate since the uses of high-power cells are continuously increasing. To develop safer separators possessing improved thermal stability and mechanical property, research efforts have been focused on hybridizing separator films/membranes with inorganic materials.[48–50] $CaCO_3$, the most abundant biomineral found in nature,[1] is a good candidate for such application according to Zhang et al.[48] The $CaCO_3$/Teflon composite membrane with a composition ratio of 92:8 (wt.%) exhibited a good capacity retention and a high-rate performance as a safety-proof battery separator in Li-ion cell. Furthermore, the alkali $CaCO_3$ also acted as a scavenger of hydrofluoric acid (HF), which is inevitably present in $LiPF_6$-based electrolyte

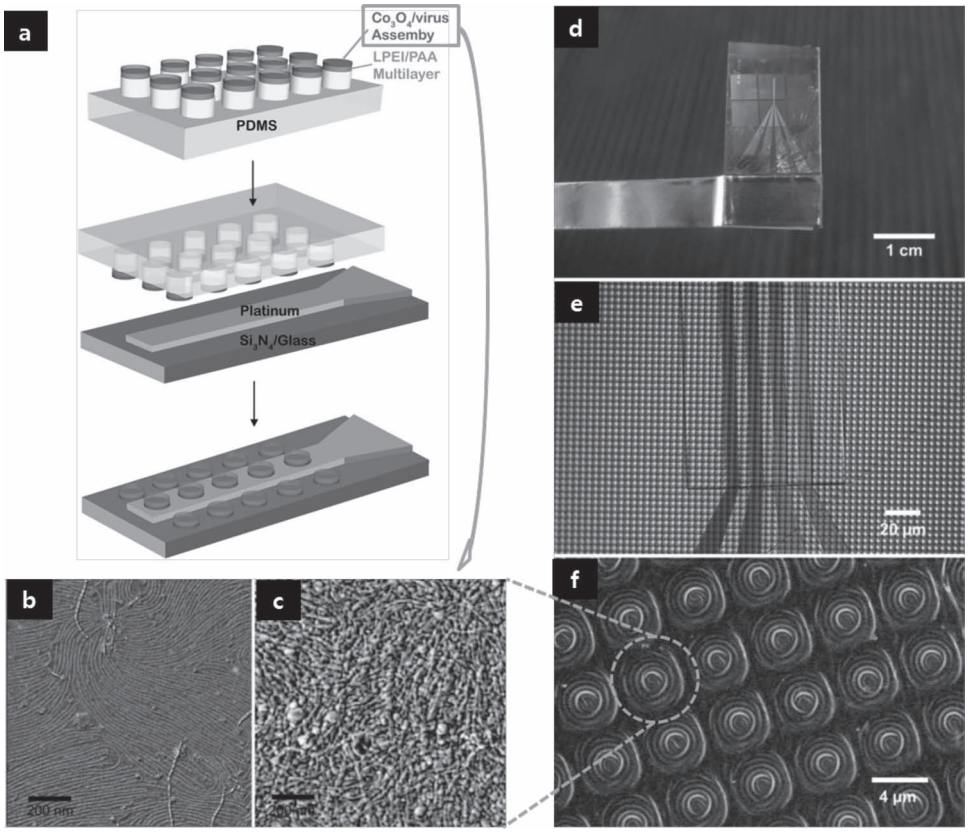

Figure 1. Construction of M13 virus based microbattery electrodes on PDMS substrate. (a) Schematic illustration of the fabrication procedure. The virus-templated cobalt oxide (Co_3O_4) nanowires were assembled on the polyelectrolyte multilayer and stamped onto Pt microband current collectors. (b, c) Phase-mode AFM images of virus assembly (b) before the Co_3O_4 growth and (c) after the Co_3O_4 growth. (d) A photograph image of microbatteries on the Pt current collector. (e) Optical microscopic image of the microbattery electrodes on four Pt microband current collectors with 10 μm width. (f) SEM image of the stamped microbattery electrodes with 4 μm diameter. Reprinted with permission.[29] Copyright 2008, National Academy of Sciences.

engendering degrade of cathode, providing an additional benefit to the rechargeable Li-ion battery as an inexpensive and safe separator film. As the needs for safe, high-power cells in electrical vehicles and energy storage system are continuously expanding, rooms exist for the application of bio-inspired strategies to fabricate safer battery separators and effective electrode materials with high-power battery performance. It is yet hard to find examples of designing electrolytes using biomimetic mineralization, probably due to the fact that most electrolytes for rechargeable batteries are Li^+ ions dissolved in liquid solvents or gel polymer matrices. Notwithstanding, bio-inspired mineralization is expected to provide novel routes to effectively designing component materials for Li-ion batteries.

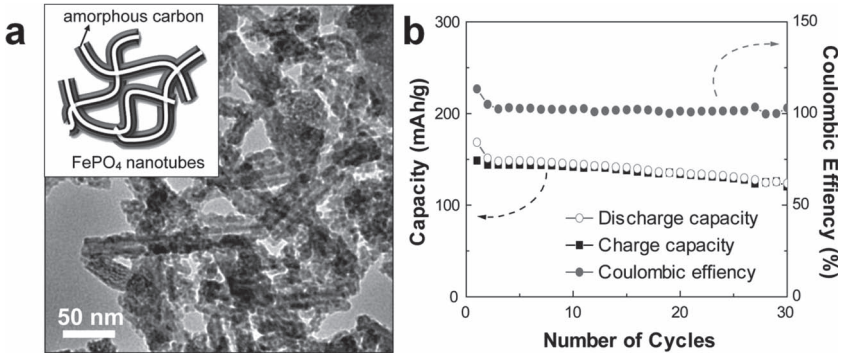

Figure 2. (a) Nanostructures of transition metal phosphates were fabricated through bio-inspired mineralization of self-assembled peptide hydrogel nanofibers. $FePO_4$-mineralized peptide nanofibers were readily converted to carbon-coated $FePO_4$ nanotubes after heat treatment. (b) $FePO_4$-mineralized peptide nanofibers exhibited a high and reversible charge/discharge capacity as Li-ion battery cathode. Reprinted with permission.[42]

2.2. CO_2-Utilizing Pathway for the Synthesis of Highly Ordered Functional Materials

The accumulation of CO_2 gas is considered as one of the main causes for the current climate change, largely resulting from the overuse of fossil fuels.[51–53] Thereby, research efforts are increasing to find eco-friendly strategies to store and utilize CO_2 gas. Biomineralization

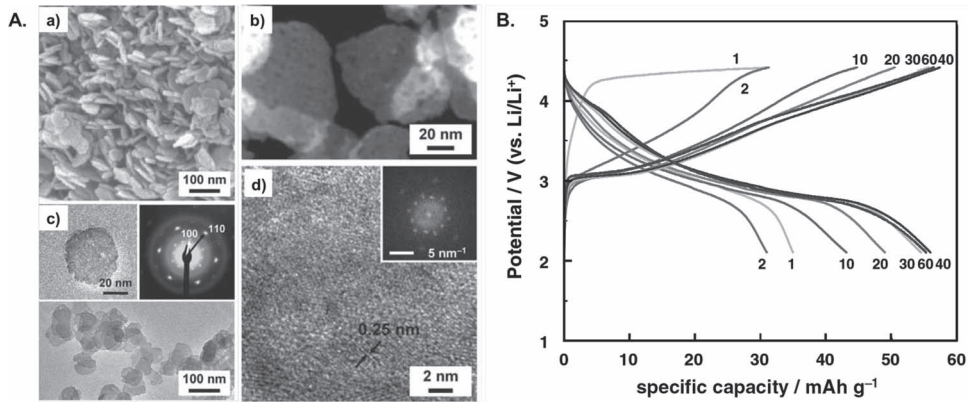

Figure 3. (A) Electron microscopy images of the β-MnOOH nanostructures prepared from the precursor solution containing ascorbic acid. (a) A SEM image. (b) A porous interior of less than 5 nm in pore size observed by HAADF-STEM. (c) TEM images with corresponding SAED pattern showing hexagonal diffraction pattern corresponding to the (100) and (110) planes of β-MnOOH. (d) A TEM image showing a series of lattice fringes corresponding to the (110) planes with the spot fast-Fourier-transform image (inset) indicating that the β-MnOOH nanostructures are presumptively mesocrystals with single crystalline architectures. (B) Charge–discharge curves of the β-MnOOH applied as a cathode material at the current density of 0.1 Ag^{-1} over the voltage range of 2.1–4.4 V vs. Li/Li^+ reference electrode. Reprinted with permission.[43]

is nature's strategy of storing and utilizing CO_2 in a form of inorganic materials. For example, a variety of marine organisms, such as mollusks, coccolithophores, and corals, convert CO_2 into convoluted structural minerals having biologic functions.[54–57] Challenges have recently been made to design materials having complex architectures and practical functions inspired by the natural pathway of converting CO_2 into biogenic materials.

2.2.1. CO_2 Injection

Recently, Kim et al.[58] succeeded in the conversion of CO_2 gas to hollow, vaterite $CaCO_3$ microspheres using dopamine (**Figure 4**), the mimetic small molecule of L-DOPA in mussel adhesive proteins.[59–61] The presence of dopamine increased the CO_2 conversion rate when CO_2 gas was injected into the mixture of $CaCl_2$ and dopamine, attributed to the facilitation of local supersaturation of Ca^{2+} by its affinitive interaction between dopamine[62] to induce faster mineralization. The microspheres could also encapsulate fluorescein isothiocyanate (FITC) by simply adding the FITC into the starting reaction mixture. The CO_2-converting pathway was utilized to produce bone-bioactive mineral/biodegradable polymer composites. The $CaCO_3$ microspheres were formed and readily converted into hydroxyapatites covering porous, polydopamine-coated electrospun polycaprolactone (E-PCL) scaffold when incubated in a simulated body fluid (SBF) at human body temperature of 37°C. Electrospun PCL scaffold is widely used for tissue ingrowth and bone regeneration.[63–65] It should be also noted that bone bioactivity of a material is typically assessed in vitro by measuring the formation rate of apatite crystals on the surface of the material in the SBF of which the pH and ion composition are nearly equal to those of human blood plasma,[66,67] as it is similar to the in vivo formation of bone crystals in hard tissues.[68–70] Thus, the CO_2-utilizing pathway may be applied for producing scaffolds for bone regeneration, simultaneously encapsulating drugs or bioactive compounds. Walsh et al.[71] showed that spheroidal vaterite structures having sponge-like morphology consisted of randomly arranged hemispherical surface depressions and pores could be formed by bubbling CO_2 gas in water-in-oil microemulsions. The microbubbles of CO_2 gas were entrapped within and at the water droplet surface containing supersaturated $Ca(HCO_3)_2$ solution and sodium dodecylsulfate (SDS) molecules present in the oil/water droplet interface. The authors anticipated such materials may find use in microcapillary devices, drug delivery systems, and biomedical implants. Wakayama et al.[72] produced $CaCO_3$-biopolymer composite thin films by means of supercritical CO_2 gas injection. They fabricated a composite bio-film of spin-coated cellulose/chitosan matrices infiltrated with densely packed vaterite particles under bubbling supercritical CO_2 gas by using polyacrylic acid (PAA) as a crystal-controlling additive. Similarly, composite films of chitosan matrices and aragonite, another crystalline form of $CaCO_3$, could also be synthesized using supercritical CO_2 gas and PAA as a crystal modifier.[73]

2.2.2. CO_2 Diffusion

Other than the direct injection of CO_2 gas, CO_2 diffusion is also a good way to produce CO_2-derived high-order structured materials. For example, a layer-by-layer assembly of polymer thin-films and $CaCO_3$ strata that resemble nacre, which will be further reviewed in the next chapter, was synthesized by a CO_2-diffusion method, where CO_2 gas diffuses from the decomposition of $(NH_4)_2CO_3$ in a closed desiccator at room temperature.[74] The CO_2-diffusion method was also applied to producing hierarchical, self-assembled architectures mimicking collagen, where one-dimensional metal-organic framework served as a template for the biomimetic mineralization of calcite.[75] Likewise, unusually shaped, higher-order structures of hierarchical calcite mesocrystals made of triangular calcite subunits with sharp edges and facets could be attained using the analogous CO_2-diffusion method.[76] Thus, the CO_2-utilizing bio-inspired strategies may provide a novel concept to cost-effective,

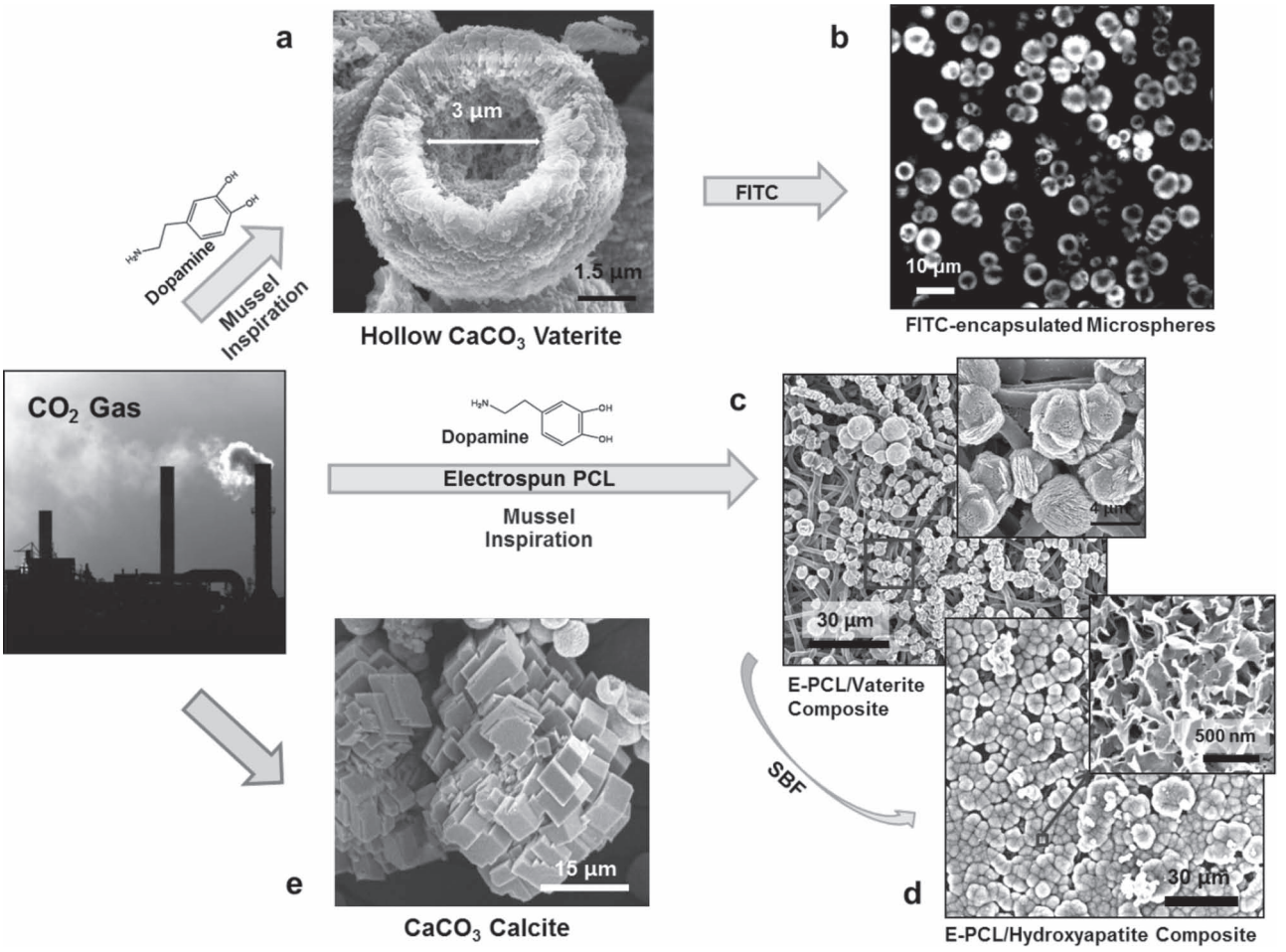

Figure 4. Schematic illustration of bio-inspired mineralization of CO_2 to hollow vaterite microspheres and biodegradable polymer/biomineral composites. (a) A hollow vaterite microsphere produced from CO_2 conversion in the presence of dopamine. (b) Hollow vaterite microspheres encapsulating FITC produced from the same method in the presence of dopamine and FITC. (c) Vaterite conspicuously formed on polydopamine-coated electrospun PCL scaffold via CO_2 conversion. (d) E-PCL/hydroxyapatite composite produced from immersing the E-PCL/vaterite composite in (c) in SBF. (e) Rhombohedral calcites formed from CO_2 conversion without dopamine. Reprinted with permission.[58] Copyright 2011, Royal Society of Chemistry.

environment-friendly fabrication of functional, high-order-structured materials.

3. Biomimetic Hybrid Structures and Carbon Composites

3.1. Tough, Strong Materials Mimicking Nacre Structure

Fracture toughness is a critical limiting parameter for designing structural materials that demand both strength and toughness.[77] This basic mechanical property is correspondingly crucial for synthesizing diverse functional materials with improved safety and stability. The nacre of a shell is an orientated coating composed of alternating layers of biomineral (i.e., $CaCO_3$ aragonite) and biopolymer (i.e., proteins). Nacre exhibits doubly harder mechanical strength and 1000-times higher toughness than its compositional phases.[78] The synthesis of materials that mimic the structure of nacre has been studied to replicate such fascinating mechanical properties; however, it is difficult to synthetically emulate nacre's architecture due to its intricately scaled structures and low organic composition.[79,80] We briefly discuss the evolution of efforts that have successfully transcribed such structures to improve structural/functional materials.

3.1.1. Nacre-Mimetic Organic-Inorganic Hybrid Hierarchy

Generally, a nacre-mimetic hierarchy can be generated through an appropriate combination of inorganic crystals and organic polymers. For example, Sellinger et al.[78] fabricated a nacre-mimetic structure composed of silica and poly(dodecylmethacrylate) (PDDMA). They developed a self-assembled process for the synthesis of nacre-mimetic, nano-laminated coatings, starting from a mixture of silica, surfactant (i.e., cetyltrimethylammonium bromide), and organic monomers (i.e., dodecylmethacrylate). The evaporation during dip-coating of the mixture induced the formation of micelles, and organic constituents were partitioned into the micellar interiors. Subsequently,

silica-surfactant-monomer micelle species self-assembled into a lyotropic mesophase, organizing the organic and inorganic precursors into a nanolaminated form. Finally, the polymerization of organic monomers fixed and completed the nacre-mimetic nanocomposite structure. A few years later, Kato et al.[81] fabricated a nacre-mimetic structure using nacre's actual component mineral (i.e., $CaCO_3$). A layer-by-layer assembly of $CaCO_3$ aragonite thin-film on a chitosan template was induced using PAA as a crystal inducer of aragonite on the surface of a flat chitosan template. PAA was also utilized as a mineralization facilitator for forming a nacre-like multilayer structure composed of $CaCO_3$ and polymers. The inorganic thin-layers of $CaCO_3$ and organic layers of polymer thin-films composed of diazo-resins and PAA were synthesized by means of CO_2 diffusion method in a closed desiccator, where CO_2 was converted to $CaCO_3$ on the PAA-present organic layers.[74] The thickness of the inorganic layer could be effectively controlled by adjusting the diffusing time of CO_2 gas. In a similar way, a hierarchical organic-inorganic structure with oriented assembly had been also synthesized through biomimetic crystallization of K_2SO_4 using PAA.[82]

3.1.2. Freezing-Pathway of Synthesizing Nacre-Mimetic Structure

Interestingly, "ice" hints at the design of nacre-mimetic materials that possess remarkably enhanced mechanical properties.[79,83,84] Ice-templated, porous layered materials were first fabricated through a freeze-casting process that included unidirectional freezing of ceramic suspensions, such as hydroxyapatite, silica, or aluminum oxide (Al_2O_3). Subsequently, this porous scaffold was filled with organic (e.g., epoxy) or metal (e.g., titanium) to construct a nacre-like composite structure.[79] The lamellar hydroxyapatite scaffold fabricated by means of the process exhibited a mechanical property four times stronger than conventional porous hydroxyapatites. Moreover, it showed well-defined pore connectivity along with directional and completely open porosity of an adequate size favorable for bone ingrowths, suggesting its feasible applications for bone substitutes. In a similar manner, a nacre-like, brick-and-mortar hybrid structure of Al_2O_3 (the brick) and polymethyl-methacrylate (PMMA, the mortar) could also be synthesized by pressing and collapsing the lamellae scaffold.[84] This synthesis also started from the above mentioned ice-templating in the direction perpendicular to the lamellar structure, followed by a further sintering step to form grafted ceramic bridges between the bricks. The bridges between the ceramic layers with rough surfaces and the presence of a submicrometer polymer film between alumina blocks enabled controlled sliding that contributed to the highly increased crack-growth toughness. Its toughness was higher than that of a lamellar structure or actual nacre, exhibiting 300 times higher toughness than its main constituent Al_2O_3.

3.1.3. Minimizing Softness

Minimizing the content of 'soft' organic components remains a difficult obstacle to replicating the actual nacre structure.[80,84] A technique that prospectively overcomes such obstacle has been recently introduced by Burghard et al..[80] They controlled the content of organic components in nacre-mimetic structure by adjusting the thickness of organic layers while depositing them using a layer-by-layer assembly of oppositely charged polyelectrolytes comprising sodium poly(styrenesulfonate) (PSS), polyethyleneimine (PEI), and poly(allylamine hydrochloride) (PAH). (**Figure 5**) They produced a layered titanium oxide (TiO_2)-polyelectrolyte composite that showed maximum

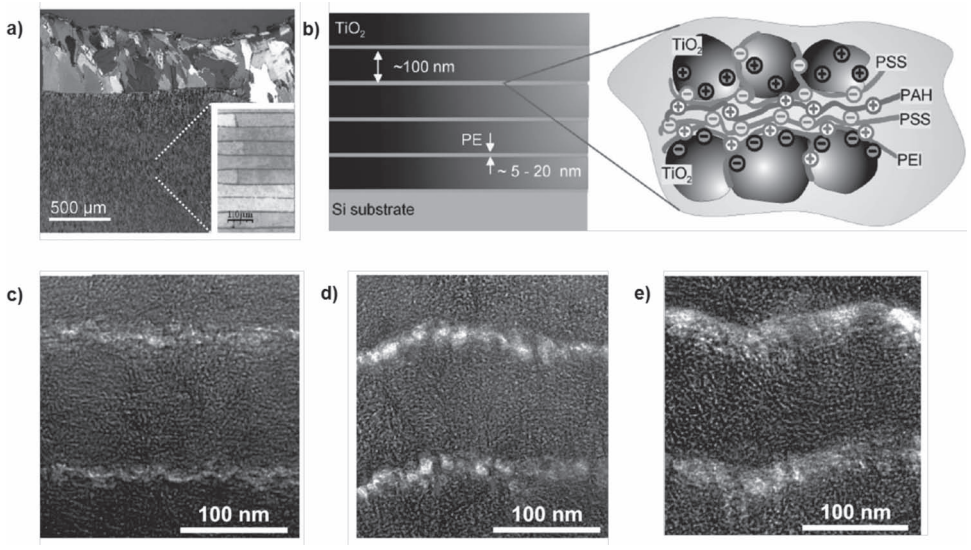

Figure 5. Schematic illustration of the nacre-like hybrid films (a, b) and high-resolution TEM images of cross-section of nacre-like hybrid film (c to e). (a) Polarized light microscope image of cross-sectional Red Abalone shell. The upper mosaic-like region is a calcite layer, while the bottom region is a nacreous layer composed of aragonite and protein. The inset is an AFM image of the nacre part where the thickness of the aragonite platelets is 400–500 nm and that of the protein layers 40–50 nm. (b) The nacre-like hybrid film is produced from a layer-by-layer assembly of TiO_2 layer and polyelectrolyte (PE) layer composed of PSS, PEI and PAH. The $(PE/TiO_2)_5$ composite film comprises a TiO_2 layer (dark) of ~100 nm thickness and a PE layer (bright) of thickness of (c) ~5 nm, (d) ~10 nm, and (e) ~20 nm. Reprinted with permission.[80] Copyright 2009, American Chemical Society.

mechanical performance at the controlled inorganic/organic thickness ratio of 10:1, which is close to that of natural nacre. Bio-inspired approaches towards enhancing mechanical properties of structural materials are still ongoing; it may not be too long before we meet an artificial, biomimetic structure that is actually stronger and tougher than the natural one.

3.2. Carbon-Biomineral Composite Materials

Carbon-based nanomaterials, namely carbon nanotubes (CNTs) and graphenes, have attracted materials scientists due to their unique mechanical strength and electric properties. These materials serve as excellent reinforcing components for composite materials, providing an effective way of producing functional materials with remarkable mechanical properties other than mimicking nacre structure. Recently, carbon hybrids with bioactive minerals are being studied to provide stiffer and stronger mechanical properties to the original mineral components for prospective applications such as reinforced medical implants.

3.2.1. Biominerals Hybridized with Carbon Nanotubes

Since the discovery of helical microtubules of graphitic carbon by Iljima et al.,[85] CNTs have been frequently applied to produce composites that possess enhanced conductivity and mechanical strength.[86] In particular, the hybridization of ceramics with CNTs has been studied to endow ceramic composites with higher stiffness and improved mechanical properties.[87] In this respect, many studies have reported on the hybridization of bioactive/bioresorbable minerals with CNTs, mainly for designing reinforced bone-implantable materials.[88–93] For instance, a laser-alloying technique was developed to fabricate hydroxyapatite-CNT composite coating on Ti-6Al-4V substrate via a metallurgical fusion bonding.[88] The results showed that increased amount of CNTs in the precursor phase improved the hardness and modulus of composite coating, which is desirable in high-load-bearing metal implants. Recently, Agarwal et al.[89] developed different methods to produce CNT-reinforced hydroxyapatite composites on Ti-6Al-4V substrate using a plasma-spray technique. According to their work, CNTs were well-dispersed in hydroxyapatite matrices (**Figure 6**A) and the composite coatings exhibited 56% increased fracture toughness compared to pure hydroxyapatite. They further developed spark plasma sintering technique to produce a CNT-hydroxyapatite composite with 92% increased fracture toughness and 25% increased elastic modulus.[91] The composite also showed enhanced wear resistance with a reduced friction coefficient that resulted from lubrication by means of delaminated graphene layers. These CNT-reinforced composites fabricated by plasma were biocompatible; they showed an unrestricted growth of human osteoblast cells near the CNT regions[89] (Figure 6B) and normal in vivo bone growth without cytotoxic effect around hydroxyapatite-CNT-coated implants embedded in rodents' bone (Figure 6C).[92] The hydroxyapatite-CNT coating exhibited good reinforcement of increased elastic modulus of the coating and adjoining freshly grown bone at the implant/bone interface (Figure 6C-c, d). On the other hand, a bio-inspired method of designing CNT-hydroxyapatite composite has been reported using mussel-adhesive-mimetic polydopamine coating.[93] Polydopamine coating on CNTs could work as an

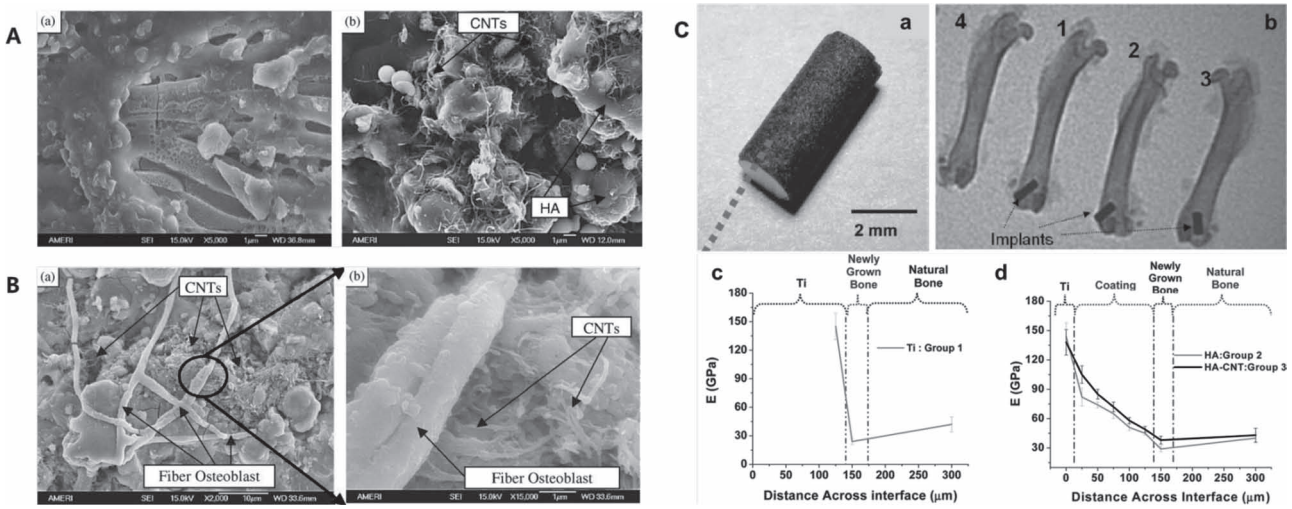

Figure 6. (A) SEM images of top-surface of plasma sprayed (a) hydroxyapatite coating without CNT and (b) hydroxyapatite-4 wt% CNT coating with uniform distribution without agglomeration on the Ti-6Al-4V substrate. (B) SEM images showing (a) unrestricted growth of human osteoblasts embedded in hydroxyapatite matrix and (b) cell-growth alongside of CNTs in vitro. (C) Hydroxyapatite-CNT coated implants in rodents' bone and its elastic modulus. Group 1 to 4 respectively indicates specimens with uncoated, hydroxyapatite coated, hydroxyapatite-CNT coated Ti implants and without implants. (a) Hydroxyapatite 4wt%/CNT coated on titanium rod. (b) X-ray image of all four groups showing good integration with the bone without osteolysis or inflammatory reactions. (c) Gradient of elastic modulus across the bone/implant interface for pure Ti implant showing a sharp change at the interface. (d) Group 2 and 3 showing gradual change in the elastic modulus at the implant/bone interface. Group 3 shows improved elastic modulus of the hydroxyapatite coating and the adjacent newly formed bone. Panel A and B were reprinted with permission.[89] Copyright 2007, Elsevier Limited. Panel C was reprinted with permission.[92] Copyright 2011, American Chemical Society.

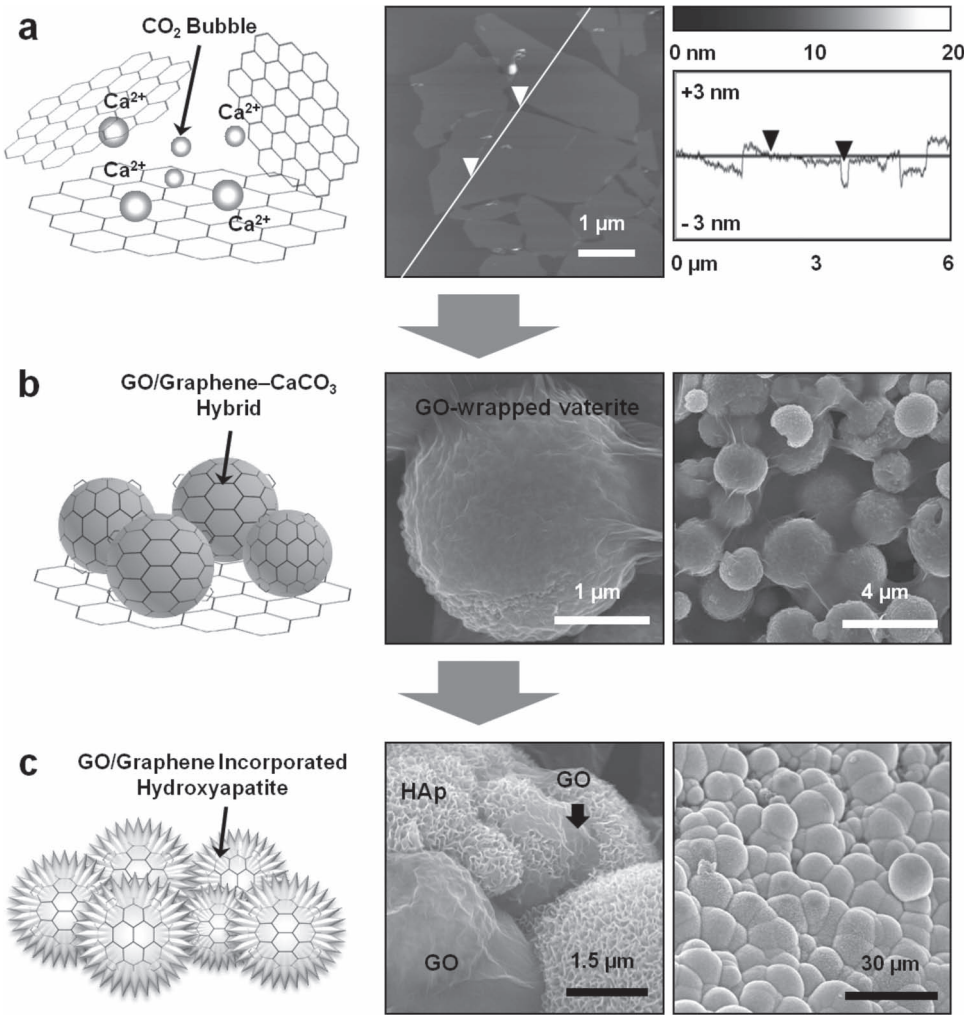

Figure 7. Syntheses of GO/graphene-biomineral hybrid materials. (a) CO_2 mineralization to $CaCO_3$ in the presence of GO sheets and $CaCl_2$. (b) GO/graphene-$CaCO_3$ hybrid materials. (c) Their conversion to GO/graphene-hydroxyapatite hybrid materials. Images on the right column show (a) AFM image and sectional analysis of GO sheets; (b) SEM images of GO-$CaCO_3$ hybrid film composed of GO-wrapped vaterite microspheres networks; (c) SEM images of GO-hydroxyapatite hybrid film that show hydroxyapatites incorporating GO sheets and covering the entire film surface. Reprinted with permission.[101]

excellent hydroxyapatite-crystallization facilitator in an SBF to produce well-mixed CNT-hydroxyapatite composite. The composite showed minimal cytotoxic effect on osteoblast cells compared to pristine CNTs. Taken together, CNTs hybridized with hydroxyapatite mineral have a potential for future applications in bone-related therapies.

3.2.2. Biominerals Hybridized with Graphene

Graphene, a sp2-bonded carbon layer of graphite with a thickness of single atom, has been gaining high interest due to its excellent thermal and mechanical properties along with its exceptional electrical conductivity.[94–97] It is also applied as a reinforcing component in various composite materials.[98–100] Recently, Kim et al.[101] reported successful hybridization of bioactive calcium-based minerals and graphene nanosheets (**Figure 7**). They fabricated biocompatible, self-standing hybrid films of graphene oxide (GO) and $CaCO_3$ vaterite by means of CO_2-injection method. Subsequent reduction of thus-formed GO-$CaCO_3$ composite produced conductive graphene-$CaCO_3$ hybrid film. The formation of vaterite microspheres and their preservation within the GO sheets is attributed to favorable interaction between Ca^{2+} in vaterite and residing functional groups of GO sheets, such as hydroxyl, epoxy, carboxylic acid, and carbonyl groups.[102–105] Strong mechanical strength of the GO network surrounding the microspheres may further hinder the dissolution of vaterite and its recrystallization to calcite.[106] The hybrid film could be readily converted to GO/graphene-incorporated hydroxyapatite when incubated in an SBF solution. The hybrid material exhibited good viability and proliferation of osteoblast cells as well, suggesting the possibility of applying graphene in bone-related clinical fields. A recent report[107] demonstrated that graphene could work as a biocompatible scaffold for the proliferation of human mesenchymal stem cells, even accelerating their specific differentiation into bone cells. Newly unveiled electrochemical[108–110]

and biological properties[111,112] of graphene are progressively expanding prospective applications. In this regard, hybridization of bone bioactive minerals (e.g., $CaCO_3$, hydroxyapatite) with carbon materials (e.g., CNTs, GOs, and graphenes) should further broaden the horizon of potential applications of bio-inspired mineralization.

4. Recent Advances in Biomedical Applications

4.1. Synthesis of Bone Bioactive Materials

The development of biomedical materials for bone (or teeth)-related clinics is one of conventional fields to which the biomimetic calcium-based minerals are most widely applied. Bone is a hierarchically structured, composite biomaterial that possesses outstanding structural and mechanical properties composed of biominerals (e.g., hydroxyapatites) and proteins (e.g., collagens).[16] The syntheses of mimetic/replaceable materials of bone or that forms bone have incessantly been studied throughout the history of biomedical applications to find treatment for various bone defects such as physically wounded or missing bones, osteoporosis, Paget's disease and hypercalcemia.[17,18]

4.1.1. Bone Bioactive Minerals and their Assessment

Inorganic materials used for bone-therapeutic applications are usually in the form of ceramics for the repair and reconstruction of diseased or damaged parts of the musculo-skeletal system. For example, Hench[113,114] viewed bone-therapeutic ceramics as bioinert (e.g., alumina, zirconia), resorbable (e.g., tricalcium phosphate), bioactive (e.g., hydroxyapatite, bioactive glasses, glass-ceramics), anticipating that the future bioceramics would be both bioactive and bioresorbable. In such regard, studies on the synthesis of bone-repairing materials are continuously advancing, often together with the purpose of simultaneously delivering bone bioactive compounds, such as bone morphogenetic protein-2 (BMP-2),[115–118] which will be more discussed later in the manuscript. The formation of hydroxyapatite, a calcium phosphate mineral that constitutes teeth and bones,[119] is considered a representative requisite for the synthesis of bone bioactive materials. The bone bioactivity is widely tested in vitro through assessing apatite formation rate in SBF, the mimetic fluid of human blood plasma with similar pH and ionic composition proposed by Kokubo et al.,[66,67] at human body temperature as mentioned earlier in the manuscript. This method is frequently performed on diverse bioceramic materials, such as bioactive glasses, to assess their bone bioactivities. Recent reports on bioactive glasses demonstrated remarkable improvements on their in vitro bone-forming activities in SBF, which is achieved by introducing highly ordered mesoporous bioactive glass structures to the SBF.[120–122]

4.1.2. Mussel-Inspired Synthesis of Bone Bioactive Minerals

A facile way of inducing in vitro bone bioactivity has been found by a unique bio-inspired strategy. Ryu et al.[123] reported that the coating of polydopamine, a biopolymer that mimics adhesive proteins secreted from mussels,[59–61] could highly facilitate the formation of hydroxyapatite on virtually any material, regardless of its type and shape. It is known that dopamine spontaneously undergoes oxidative polymerization in an aqueous solution to become polydopamine, which exhibits a strong universal adhesive property to various substrates.[59–61] Abundant catechol groups in polydopamine coating concentrate Ca^{2+} ions onto the coating layer and promote the formation of hydroxyapatite (**Figure 8**). According to a recent study,[124] dopamine is non-toxic to osteoblast cells and even facilitates cell adhesion by enhancing substrate attachment, spreading, and cytoskeleton development. Meanwhile, Kim and Park reported that dopamine can stabilize the formation of $CaCO_3$ vaterite microspheres.[125,126] Note that vaterite is a metastable crystalline phase of $CaCO_3$ under its rapid, spontaneous transition in aqueous state from an amorphous phase (i.e., amorphous calcium carbonate or ACC) to rhombohedral calcite, the stable phase. They further demonstrated that vaterite microspheres stabilized by dopamine exhibited highly enhanced transformation into carbonated hydroxyapatites in SBF.[126] Both stabilization of vaterite and transformation to hydroxyapatite were significantly diminished in lower (0.1x) concentration of dopamine. The stabilization of vaterite is attributed to dopamine, which favorably interacts with Ca^{2+} ions within vaterite and prevents the dissolution/recrystallization-to-calcite process. The presence of dopamine further concentrates Ca^{2+} ions in SBF to the vaterite surface, facilitating the transformation of carbonated hydroxyapatites starting from the surface. Carbonated hydroxyapatites are more similar to biologic apatites and show better biocompatibility and bioresorption rate compared to pure hydroxyapatites.[18,70] Besides, polydopamine coatings can deposit Au and Ag nanoparticles on its surface through a redox process, which can endow anti-bacterial property to the material.[127,128] Thus, the mussel adhesion-inspired strategies of producing bone minerals suggest a simple, versatile and effective route to synthesizing bone bioactive materials.

4.2. Biominerals as a Carrier for Drug Delivery Systems

Calcium-based minerals (or their composites) have been also widely studied as carriers for the delivery of drugs, proteins, and many other bioactive compounds. Hydroxyapatites and $CaCO_3$ are the popular minerals used for such applications as they are highly porous, biocompatible, and biodegradable.[129–135] They are often closely associated with curing bone defects by delivering the anti-inflammatory drugs or bone-bioactive compounds.

4.2.1. Protein Carriers

Proteins, such as bovine serum albumin (BSA),[129,135,136] hydrophobin,[137] and BMP-2s or its derivative peptides[115–118] were successfully incorporated into hydroxyapatites for their deliveries. Especially, the encapsulation of BMP-2s in hydroxyapatites and their deliveries were studied for orthopedic or bone regeneration purposes. For example, BMP-2s were successfully incorporated into hydroxyapatite scaffolds that are hybridized

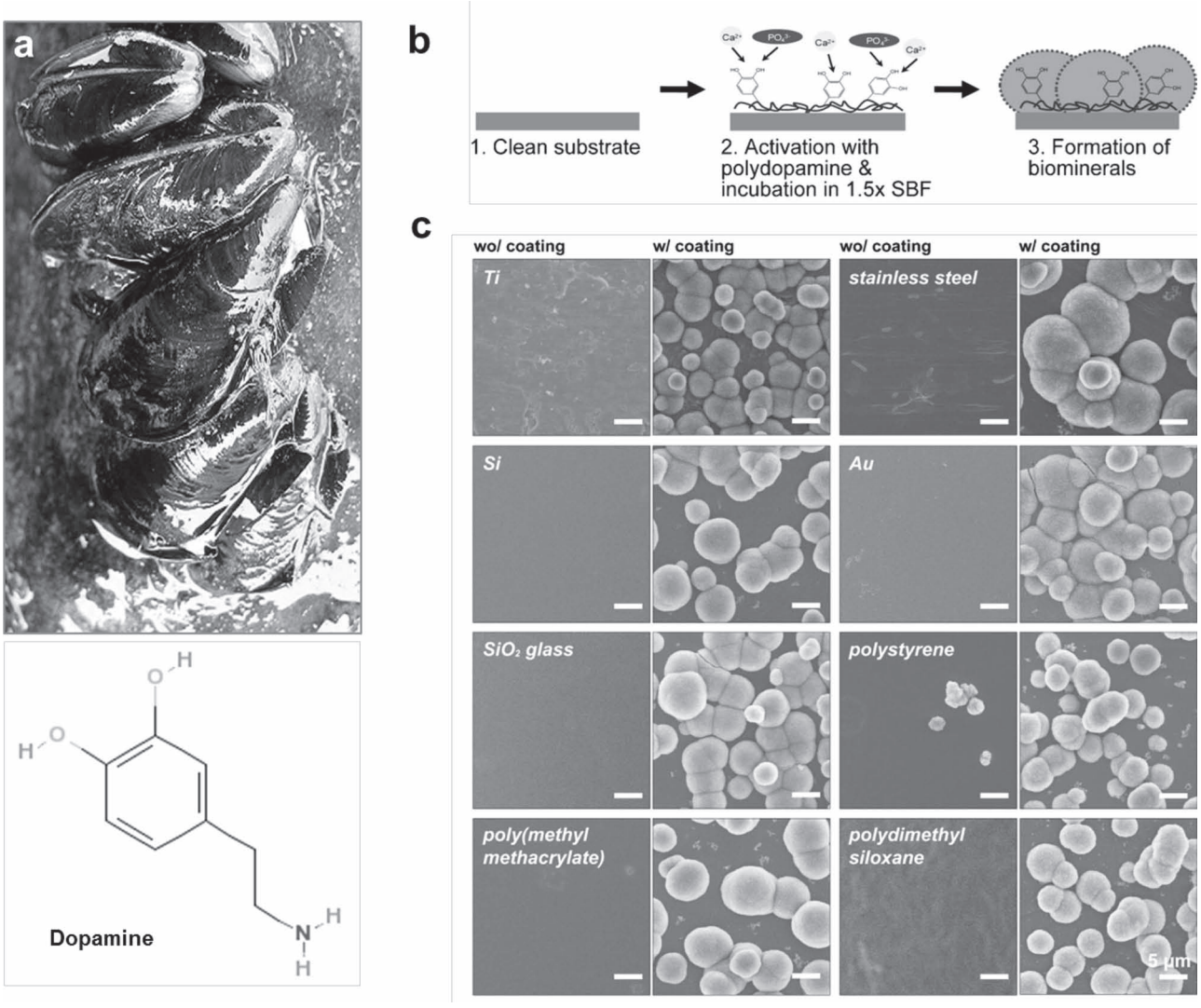

Figure 8. Mussel adhesion-inspired calcium phosphate crystal formation. (a) Chemical structure of dopamine. (b) Scheme for polydopamine-assisted calcium phosphate crystal formation. (c) Hydroxyapatite formation on various polydopamine-coated flat solid substrates of metals (i.e., Ti, stainless steel), metalloids (i.e., Si), noble metals (i.e., Au), ceramics (i.e., SiO_2 glass) and polymers (i.e., PMMA, PDMS). The scale bar represents 5 μm. Panel (b) and (c) are reprinted with permission.[123]

with biodegradable polymers, such as poly(lactic-co-glycolic acid) (PLGA), and released in a controlled manner.[115,117] Furthermore, the incorporation of hydroxyapatite into an electrospun PLGA matrix could enhance the attachment and viability of human marrow-derived messenchymal stem cells in vitro.[115] The bioactivity of BMP-2 released from hydroxyapatite-PLGA composite microspheres was well maintained, further enhancing the healing and substitution of osteonecrotic bone in vivo.[117]

4.2.2. Anti-Inflammatory Drug Carriers

Hydroxyapatites can also be utilized for the drug delivery media for curing bone infection or inflammatory responses. For instance, PerOssal®, a commercially available bioresorbable composite of nanoparticulate hydroxyapatite and calcium sulfate ($CaSO_4$), exhibited higher release rate of vancomycin and lesser cytotoxicity than bare $CaSO_4$.[132] Hydroxyapatites that were functionalized with hydroxypropyl-β-cyclodextrin polymer exhibited increased initial burst and prolonged release of antibiotics including vancomycin and ciprofloxacin, compared to non-functionalized hydroxyapatites.[138] Hollow, ellipsoidal hydroxyapatite capsules that have high specific surface area, storage capacity, and enhanced drug (i.e., ibuprofen) release property could be fabricated using $CaCO_3$ as a sacrificial template.[139] Hydroxyapatites could further be functionalized for monitoring the drug release profile.[140,141] Mesoporous structures of hydroxyapatite-strontium compound[140] and hydroxyapatite-xeolite (MCM-48) composites[141] showed blue luminescence that resulted from $CO_2\cdot$ radical impurities in their crystal lattices. The blue luminescence enabled the monitoring of the release profile of drugs, such as ibuprofen and captopril. On the other hand, the well-ordered mesoporous

bioactive glasses also showed a possible application in treating bone infection.[121] They showed accelerated conversion to hydroxyapatite in SBF in addition to the improved loading and release of gentamicin owing to their high specific area, indicating a good feasibility as an anti-inflammatory drug delivery system for preparation of bone-implantable materials.

4.2.3. Anti-Cancer Drug Carriers

Recent reports further demonstrate hydroxyapatites and $CaCO_3$ can be used for delivering anti-cancer drugs.[131,139,142–146] Hydroxyapatite nanocrystals with different shapes (e.g., plate, needle) showed different affinity to specific kinds of anti-cancer Pt-complex drugs such as cis-diammmedichloroplatinum(II) and di(ethylenediamine-platinum) medronate, with bisphosphonate alendronate, an approved clinical material for bone defects.[142] Their underlying ligand exchange or electrostatic interaction resulted in different adsorption and desorption properties, which suggests that the production of hydroxyapatite-biomolecule conjugates tailored for specific therapeutic applications can be modulated by the properties of hydroxyapatite nanocrystals. This concept was further applied to the production of an implantable, biomimetic hydroxyapatite having anti-cancer activity, which acts as both a bone substitute and a drug-releasing agent for inhibiting the growth of bone tumors.[143] On the other hand, porous $CaCO_3$ was used as an excellent loader for anticancer drugs, such as doxorubicin (DOX).[131,139,144–146] Hierarchical, hollow $CaCO_3$ particles adequately incorporated DOX and facilitated localizing drug release through their pH-sensitive structure. They enhanced cytotoxicity against cancer cells by increasing cellular uptake, perinuclear accumulation, and nuclear entry (**Figure 9**).[144] $CaCO_3$ mesocrystals could also serve as superparamagnetic carriers for co-delivery of DOX and gene nanoparticles for targeted cancer therapy.[131] In the study, $CaCO_3$ mesocrystals encapsulated Au-DNA and Fe_3O_4@silica nanoparticles for magnetic control and therapy. The nanoparticles–$CaCO_3$ hybrid material protected functional moieties from degradation and phagocytosis during blood circulation. DOX and Au-DNA were gradually released from the capsule towards targeted tissue after particle margination in vascular walls. Another study showed that $CaCO_3$ microspheres hybridized with carbomethyl chitosan (CMC) could effectively load and release water-soluble anticancer drugs (e.g., DOX-HCl).[145] It demonstrated a controllability over the size of the delivery media by adjusting the concentration of mineralizing agent: $CaCl_2$ and Na_2CO_3.(i.e., higher the concentration, larger the size under same concentration of CMC.) $CaCO_3$ microspheres could also be used as templates for producing hollow, mesoporous silica spheres (HMS) preloaded with DOX (**Figure 10**).[146] They showed efficient protection and pH-sensitive release of DOX with an enhanced intracellular delivery as well. The use of $CaCO_3$ as a sacrificial template to synthesize drug encapsulants by further mineralization of different inorganic compounds[146–150] or layer-by-layer assembly of other substances[129,130,151–157] is now a popular strategy in drug delivery systems.

5. Summary and Perspectives

Applications of bio-inspired mineralization are continuously expanding its horizons to diverse fields of science and engineering. Essential component materials of Li-ion batteries (e.g., cathode, anode and separator) have been successfully synthesized by biomimetic mineralization strategies. Bio-inspired routes to utilizing CO_2 gas were suggested to produce elaborately structured functional materials. The pursuit of fabricating tougher and stronger materials is ongoing by mimicking the structure of nacre produced by natural biogenic mineralization. Hybrid materials of bioactive minerals and carbon-based nanomaterials (e.g., CNT, GO, and graphene) hint at latent applications in future bone treatment; yet, their applications are unlimited considering the fascinating electrochemical and mechanical properties of carbon-based nanomaterials. Studies on biomedical applications are constantly

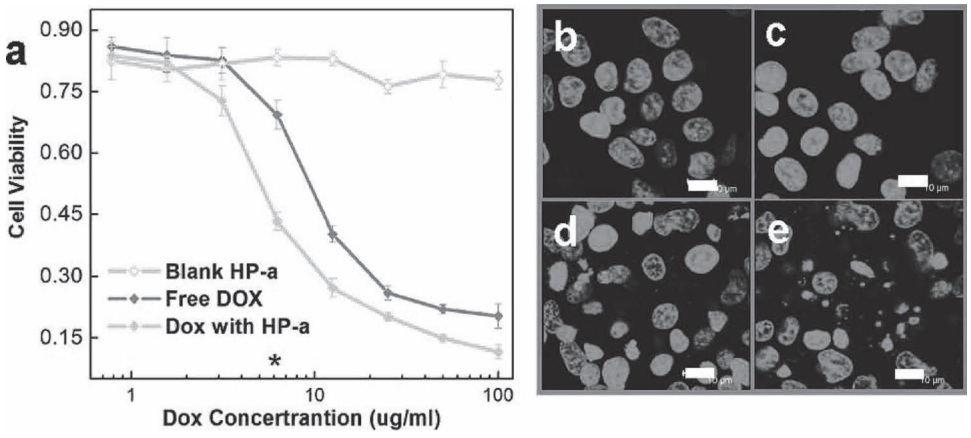

Figure 9. (a) Cytotoxicity of liver carcinoma HepG2 cells exposed to free DOX, blank HP-a, and DOX loaded HP-a for 48 h. Nuclei of (b) original HepG2 cells and the HepG2 cells incubated with (c) blank HP-a, (d) free DOX, and (e) DOX loaded HP-a after 48 h. The concentrations of additives used in (b) to (e) were corresponding to the starmarked point in (a) (scale bar: 10 μm, hierarchical particles of $CaCO_3$ spheres with ~500 nm diameter were prepared at 30 °C denoted as HP-a). Reprinted with permission.[144] Copyright 2008, American Chemical Society.

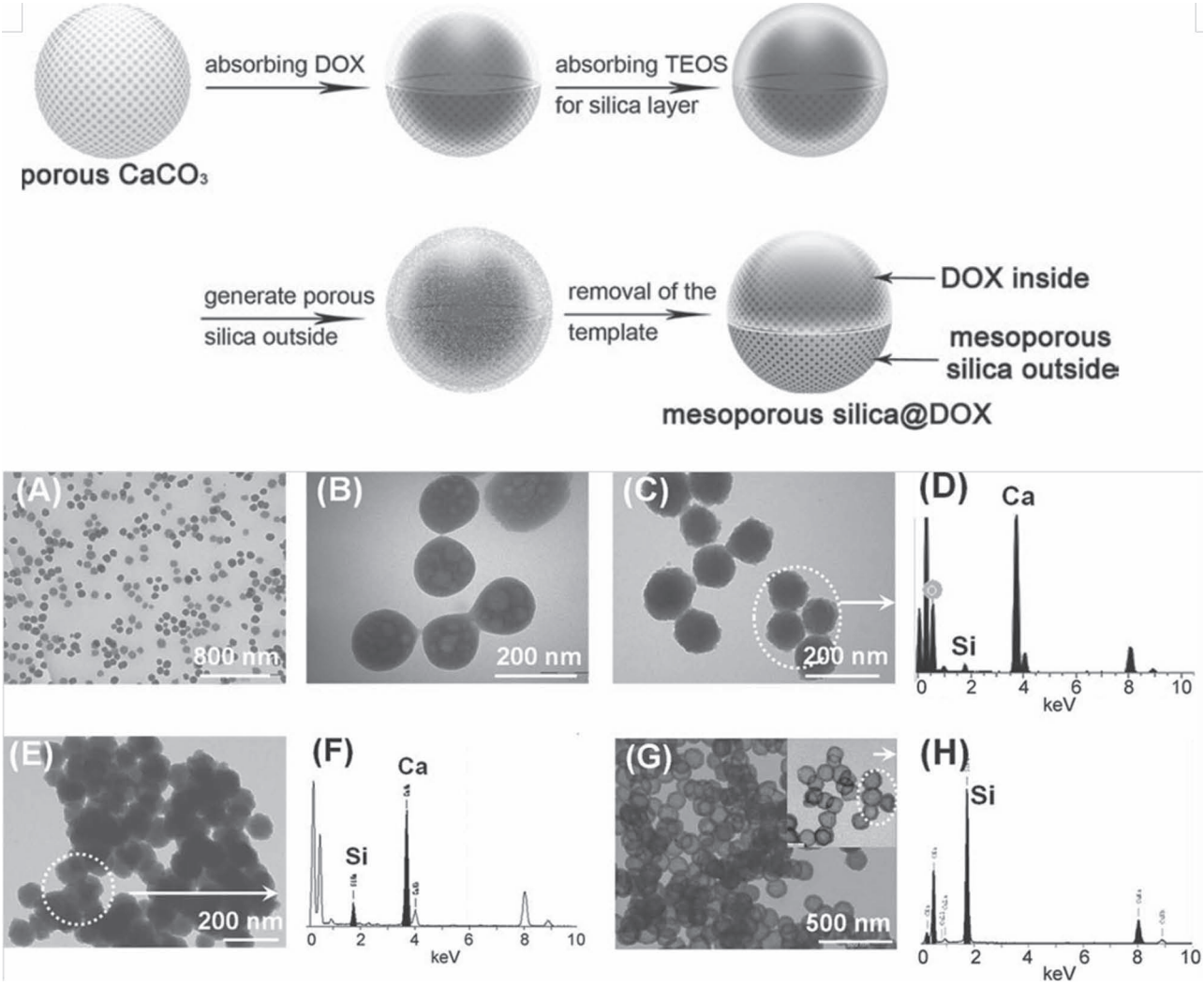

Figure 10. Schematic illustration (upper panel) and electron microscopic images with energy dispersive spectroscopy (EDS) (lower panel) for the preparation of hollow mesoporous silica (HMS) loaded with DOX (HMS@DOX) using $CaCO_3$ template. (A, B) TEM images of $CaCO_3$ nanospheres. (C) TEM image of HMS@DOX with silica layers after absorbing DOX and tetraethoxysilane (TEOS) and (D) its EDS showing peaks for Ca and trace Si. (E) TEM image of HMS@DOX after synthesis of mesoporous silica layer before removal of $CaCO_3$ template and (F) its EDS showing increased intensity peak for Si. (G) TEM images of HMS@DOX nanospheres after removal of the $CaCO_3$ template and (H) their EDS showing only peak for Si. Reprinted with permission.[146]

under progress to provide materials with better bone bioactivity through the introduction of more versatile and facile methodologies. Drug carriers have been synthesized through calcium-based minerals to efficiently load and release bioactive compounds such as proteins, antibiotics, and anticancer drugs in a controllable manner for practical therapeutic uses. The combination of these bio-inspired applications may further pioneer novel, effective approach of synthesizing advanced functional materials.

Acknowledgements

This study was supported by grants from the National Research Foundation (NRF) via National Research Laboratory (R0A-2008-000-20041-0), Converging Research Center (2009-0082276), and Intelligent Synthetic Biology Center of Global Frontier Project (2011-0031957).

Received: July 17, 2012
Published online: September 3, 2012

[1] S. Mann, *Biomineralization: Principles, Concepts in Bioinorganic Materials Chemistry*, Oxford University Press, Oxford, UK **2001**.
[2] H. A. Lowenstam, S. Weiner, *On Biomineralization*, Oxford University Press, New York **1989**.
[3] S. Mann, *Angew. Chem. Int. Ed.* **2000**, *39*, 3392.
[4] L. Addadi, S. Weiner, *Angew. Chem. Int. Ed.* **1992**, *31*, 153.
[5] S. Mann, *Nature* **1993**, *365*, 499.
[6] S. Mann, *J. Mater. Chem.* **1995**, *5*, 935.
[7] S. Mann, D. D. Archibald, J. M. Didymus, T. Douglas, B. R. Heywood, F. C. Meldrum, N. J. Reeves, *Science* **1993**, *261*, 1286.

[8] H. Cölfen, *Curr. Opin. Colloid Interface Sci.* **2003**, *8*, 23.
[9] H. Cölfen, S. Mann, *Angew. Chem. Int. Ed.* **2003**, *42*, 2350.
[10] F. C. Meldrum, H. Cölfen, *Chem. Rev.* **2008**, *108*, 4332.
[11] S. H. Yu, H. Cölfen, *J. Mater. Chem.* **2004**, *14*, 2124.
[12] S. A. Davis, M. Breulmann, K. H. Rhodes, B. Zhang, S. Mann, *Chem. Mater.* **2001**, *13*, 3218.
[13] N. Kröger, K. H. Sandhage, *MRS Bull.* **2010**, *35*, 122.
[14] B. L. Smith, T. E. Schäffer, M. Viani, J. B. Thompson, N. A. Frederick, J. Kindt, A. Belcher, G.D. Stucky, D. E. Morse, P. K. Hansma, *Nature* **1999**, *399*, 761.
[15] J. Aizenberg, J. C. Weaver, M. S. Thanawala, V. C. Sundar, D. E. Morse, P. Fratzl, *Science* **2005**, *309*, 275.
[16] S. Weiner, H. D. Wagner, *Annu. Rev. Mater. Sci.* **1998**, *28*, 271.
[17] T. A. Taton, *Nature* **2001**, *412*, 491.
[18] R. Z. LeGeros, *Chem. Rev.* **2008**, *108*, 4742.
[19] W.-Q. Yan, T. Nakamura, M. Kobayashi, H.-M. Kim, F. Miyaji, T. Kokubo, *J. Biomed. Mater. Res.* **1997**, *37*, 267.
[20] H. Ohgushi, M. Okumura, T. Yoshikawa, K. Inoue, N. Senpuku, S. Tamai, *J. Biomed. Mater. Res.* **1992**, *26*, 885.
[21] G. Daculsi, *Biomaterials* **1998**, *19*, 1473.
[22] S. Larsson, T. W. Bauer, *Clin. Orthop. Relat. Res.* **2002**, *395*, 23.
[23] G. Balasundaram, T. J. Webster, *Nanomedicine* **2006**, *1*, 169.
[24] M. Winter, R. J. Brodd, *Chem. Rev.* **2004**, *104*, 4245.
[25] M. S. Whittingham, *Chem. Rev.* **2004**, *104*, 4271.
[26] R. Pitchai, V. Thavasi, S. G. Mhaisalkar, S. Ramakrishna, *J. Mater. Chem.* **2011**, *21*, 11040.
[27] Y. J. Lee, H. Yi, W.-J, Kim, K. Kang, D. S. Yun, M. S. Strano, G. Ceder, A. M. Belcher, *Science* **2009**, *324*, 1051.
[28] Y. J. Lee, A. M. Belcher, *J. Mater. Chem.* **2011**, *21*, 1033.
[29] K. T. Nam, R. Wartena, P. J. Yoo, F. W. Liau, Y. J. Lee, Y.-M. Chiang, P. T. Hammond, A. M. Belcher, *Proc. Natl. Acad. Sci. USA* **2008**, *105*, 17227.
[30] Y. J. Lee, Y. Lee, D. Oh, T. Chen, G. Ceder, A. M. Belcher, *Nano Lett.* **2010**, *10*, 2433.
[31] S. Zhang, *Nat. Biotechnol.* **2003**, *21*, 1171.
[32] X. Gao, H. Matsui, *Adv. Mater.* **2005**, *17*, 2037.
[33] L. Niu, X. Chen, S. Allen, S. J. B. Tendler, *Langmuir* **2007**, *23*, 7443.
[34] M. Yemini, M. Reches, J. Rishpon, E. Gazit, *Nano Lett.* **2005**, *5*, 183.
[35] J. Ryu, S. Y. Lim, C. B. Park, *Adv. Mater.* **2009**, *21*, 1577.
[36] J. Ryu, C. B. Park, *Biotechnol. Bioeng.* **2010**, *105*, 221.
[37] M. Reches, E. Gazit, *Science* **2003**, *300*, 625.
[38] J. Ryu, C. B. Park, *Adv. Mater.* **2008**, *20*, 3754.
[39] X. Yan, Q. He, K. Wang, L. Duan, Y. Cui, Y. Li, *Angew. Chem. Int. Ed.* **2007**, *46*, 2431.
[40] X. Yan, Y. Cui, Q. He, K. Wang, J. Li, *Chem. Mater.* **2008**, *20*, 1522.
[41] A. M. Smith, R. J. Williams, C. Tang, P. Coppo, R. F. Collins, M. L. Turner, A. Saiani, R. V. Ulijn, *Adv. Mater.* **2008**, *20*, 37.
[42] J. Ryu, S.-W. Kim, K. Kang, C. B. Park, *Adv. Mater.* **2010**, *22*, 5537.
[43] M. Oba, Y. Oaki, H. Imai, *Adv. Funct. Mater.* **2010**, *20*, 4279.
[44] B. M. Tebo, H. A. Johnson, J. K. McCarthy, A. S. Templeton, *Trends Microbiol.* **2005**, *13*, 421.
[45] B. M. Tebo, J. R. Bargar, B. G. Clement, G. J. Dick, K. J. Murray, D. Parker, R. Verity, S. M. Webb, *Annu. Rev. Earth Planet. Sci.* **2004**, *32*, 287.
[46] H. Uchiyama, E. Hosono, H. Zhou, H. Imai, *J. Mater. Chem.* **2009**, *19*, 4012.
[47] P. Arora, Z. Zhang, *Chem. Rev.* **2004**, *104*, 4419.
[48] S. S. Zhang, K. Xu, T. R. Jow, *J. Power Sources* **2005**, *140*, 361.
[49] D. Takemura, S. Aihara, K. Hamano, M. Kise, T. Nishimura, H. Urushibata, H. Yoshiyasu, *J. Power Sources* **2005**, *146*, 779.
[50] H.-S. Jeong, D.-W. Kim, Y. U. Jeong, S.-Y. Lee, *J. Power Sources* **2010**, *195*, 6116.
[51] T. R. Karl, K. E. Trenberth, *Science* **2003**, *302*, 1719.
[52] N. MacDowell, N. Florin, A. Buchard, J. Hallett, A. Galindo, G. Jackson, C. S. Adjiman, C. K. Williams, N. Shah, P. Fennell, *Energy Environ. Sci.* **2010**, *3*, 1645.
[53] Q. Wang, J. Luo, Z. Zhong, A. Borgna, *Energy Environ. Sci.* **2011**, *4*, 42.
[54] R. A. Feely, C. L. Sabine, K. Lee, W. Berelson, J. Kleypas, V. J. Fabry, F. J. Millero, *Science* **2004**, *305*, 362.
[55] K. G. Schulz, I. Zondervan, L. J. A. Gerringa, K. R. Timmermans, M. J. W. Veldhuis, U. Riebesell, *Nature* **2004**, *430*, 673.
[56] J. A. Kleypas, R. W. Buddemeier, D. Archer, J.-P. Gattuso, C. Langdon, B. N. Opdyke, *Science* **1999**, *284*, 118.
[57] M. D. Iglesias-Rodriguez, P. R. Halloran, R. E. M. Rickaby, I. R. Hall, E. Colmenero-Hidalgo, J. R. Gittins, D. R. H. Green, T. Tyrrell, S. J. Gibbs, P. Von Dassow, E. Rehm, E. V. Armbrust, *Science* **2008**, *320*, 336.
[58] S. Kim, J. W. Ko, C. B. Park, *J. Mater. Chem.* **2011**, *21*, 11070.
[59] H. Lee, N. F. Scherer, P. B. Messersmith, *Proc. Natl. Acad. Sci. USA* **2006**, *103*, 12999.
[60] H. Lee, S. M. Dellatore, W. M. Miller, P. B. Messersmith, *Science* **2007**, *318*, 426.
[61] J. H. Waite, *Nat. Mater.* **2008**, *7*, 8.
[62] N. Holten-Anderson, T. E. Mates, M. S. Toprak, G. D. Stucky, F. W. Zok, J. H. Waite, *Langmuir* **2009**, *25*, 3323.
[63] H. Yoshimoto, Y. M. Shin, H. Teraia, J. P. Cacanti, *Biomaterials* **2003**, *24*, 2077.
[64] A. G. A. Coombes, S. C. Rizzi, M. Williamson, J. E. Barralet, S. Downes, W. A. Wallace, *Biomaterials* **2004**, *25*, 315.
[65] J.-H. Jang, O. Castano, H.-W. Kim, *Adv. Drug Delivery Rev.* **2009**, *61*, 1065.
[66] T. Kokubo, H. Kushitani, S. Sakka, T. Kitsugi, T. Yamamuro, *J. Biomed. Mater. Res.* **1990**, *24*, 721.
[67] T. Kokubo, H. Takadama, *Biomaterials* **2006**, *27*, 2907.
[68] D. K. Nagesha, M. A. Whitehead, J. L. Coffer, *Adv. Mater.* **2005**, *17*, 921.
[69] Q. Shi, J. Wang, J. Zhang, J. Fan, G. D. Stucky, *Adv. Mater.* **2006**, *18*, 1038.
[70] W. L. Suchanek, P. Shuk, K. Byrappa, R. E. Riman, K. S. TenHuisen, *Biomaterials* **2002**, *23*, 699.
[71] D. Walsh, B. Lebeau, S. Mann, *Adv. Mater.* **1999**, *11*, 324.
[72] H. Wakayama, S. R. Hall, S. Mann, *J. Mater. Chem.* **2005**, *15*, 1134.
[73] T. Iwatsubo, K. Sumaru, T. Kanamori, T. Yamaguchi, T. Sinbo, *J. Appl. Polym. Sci.* **2004**, *91*, 3627.
[74] H. Wei, N. Ma, F. Shi, Z. Wang, X. Zhang, *Chem. Mater.* **2007**, *19*, 1974.
[75] S. Burazerovic, J. Gradinaru, J. Pierron, T. R. Ward, *Angew. Chem. Int. Ed.* **2007**, *46*, 5510.
[76] A.-W. Xu, M. Antonietti, S.-H. Yu, H. Cölfen, *Adv. Mater.* **2008**, *20*, 1333.
[77] M. E. Launey, R. O. Ritchie, *Adv. Mater.* **2009**, *21*, 2103.
[78] A. Sellinger, P. M. Weiss, A. Nguyen, Y. Lu, R. A. Assink, W. Gong, C. J. Brinker, *Nature* **1998**, *394*, 256.
[79] S. Deville, E. Saiz, R. K. Nalla, A. P. Tomsia, *Science* **2006**, *311*, 515.
[80] Z. Burghard, L. Zini, V. Srot, P. Bellina, P. A. Van Aken, J. Bill, *Nano Lett.* **2009**, *9*, 4103.
[81] T. Kato, *Adv. Mater.* **2000**, *12*, 1543.
[82] Y. Oaki, H. Imai, *Angew. Chem. Int. Ed.* **2005**, *44*, 6571.
[83] J. Halloran, *Science* **2006**, *311*, 479.
[84] E. Munch, M. E. Launey, D. H. Alsem, E. Saiz, A. P. Tomsia, R. O. Ritchie, *Science* **2008**, *322*, 1516.
[85] S. Iijima, *Nature* **1991**, *354*, 56.
[86] R. H. Baughman, A. A. Zakhidov, W. A. de Heer, *Science* **2002**, *297*, 787.
[87] F. Lupo, R. Kamalakaran, C. Scheu, N. Grobert, M. Ruhle, *Carbon* **2004**, *42*, 1995.

[88] Y. Chen, Y. Q. Zhang, T. H. Zhang, C. H. Gan, C. Y. Zheng, G. Yu, *Carbon* **2006**, *44*, 37.
[89] K. Balani, R. Anderson, T. Laha, M. Andara, J. Tercero, E. Crumpler, A. Agarwal, *Biomaterials* **2007**, *28*, 618.
[90] I. Armentano, M. A. Álvarez-Pérez, B. Carmona-Rodríguez, I. Gutiérrez-Ospina, J. M. Kenny, H. Arzate, *Mater. Sci. Eng., C* **2008**, *28*, 1522.
[91] D. Lahiri, V. Singh, A. K. Keshri, S. Seal, A. Agarwal, *Carbon* **2010**, *48*, 3103.
[92] S. Facca, D. Lahiri, F. Fioretti, N. Messadeq, D. Mainard, N. Benkirane-Jessel, A. Agarwal, *ACS Nano* **2011**, *5*, 4790.
[93] M. Lee, S. H. Ku, J. Ryu, C. B. Park, *J. Mater. Chem.* **2010**, *20*, 8848.
[94] K. S. Novoselov, A. K. Geim, S. V. Morozov, D. Jiang, Y. Zhang, S. V. Dubonos, I. V. Grigorieva, A. A. Firsov, *Science* **2004**, *306*, 666.
[95] A. K. Geim, K. S. Novoselov, *Nat. Mater.* **2007**, *6*, 183.
[96] A. H. Castro Neto, F. Guinea, N. M. R. Peres, K. S. Novoselov, A. K. Geim, *Rev. Mod. Phys.* **2009**, *81*, 109.
[97] Y. Kopelevich, P. Esquinazi, *Adv. Mater.* **2007**, *19*, 4559.
[98] S. Stankovich, D. A. Dikin, G. H. B. Dommett, K. M. Kohlhaas, E. J. Zimney, E. A. Stach, R. D. Piner, S. T. Nguyen, R. S. Ruoff, *Nature* **2006**, *442*, 282.
[99] M. J. Allen, V. C. Tung, R. B. Kaner, *Chem. Rev.* **2010**, *110*, 132.
[100] Y. Si, E. T. Samulski, *Nano Lett.* **2008**, *8*, 1679.
[101] S. Kim, S. H. Ku, S. Y. Lim, J. H. Kim, C. B. Park, *Adv. Mater.* **2011**, *23*, 2009.
[102] W. Gao, L. B. Alemany, L. Ci, P. M. Ajayan, *Nat. Chem.* **2009**, *1*, 403.
[103] F. Liu, T. S. Seo, *Adv. Funct. Mater.* **2010**, *20*, 1930.
[104] S. Park, R. S. Ruoff, *Nat. Nanotechnol.* **2009**, *4*, 217.
[105] D. Li, M. B. Müller, S. Gilje, R. B. Kaner, G. G. Wallace, *Nat. Nanotechnol.* **2008**, *3*, 101.
[106] W. Li, C. Gao, *Langmuir* **2007**, *23*, 4575.
[107] T. R. Nayak, H. Andersen, V. S. Makam, C. Khaw, S. Bae, X. Xu, P.-L. R. Ee, J.-H. Ahn, B. H. Hong, G. Pastorin, B. Özyilmaz, *ACS Nano* **2011**, *5*, 4670.
[108] M. D. Stoller, S. Park, Z. Yanwu, J. An, R. S. Ruoff, *Nano Lett.* **2008**, *8*, 3498.
[109] S.-M. Paek, E. Yoo, I. Honma, *Nano Lett.* **2009**, *9*, 72.
[110] L. Tang, Y. Wang, Y. Li, H. Feng, J. Lu, J. Li, *Adv. Funct. Mater.* **2009**, *19*, 2782.
[111] Z. Liu, J. T. Robinson, X. Sun, H. Dai, *J. Am. Chem. Soc.* **2008**, *130*, 10876.
[112] C. X. Guo, X. T. Zheng, Z. S. Lu, X. W. Lou, C. M. Li, *Adv. Mater.* **2010**, *22*, 5164.
[113] L. L. Hench, *J. Am. Ceram. Soc.* **1998**, *81*, 1705.
[114] L. L. Hench, J. M. Polak, *Science* **2002**, *295*, 1014.
[115] H. Nie, W. S. Beng, Y.-C. Fu, C.-H. Wang, *Biotechnol. Bioeng.* **2008**, *99*, 223.
[116] X. Niu, Q. Feng, M. Wang, X. Guo, Q. Zheng, *J. Controlled Release* **2009**, *134*, 111.
[117] C.-K. Wang, M.-L. Ho, G.-J. Wang, J.-K. Chang, C.-H. Chen, Y.-C. Fu, H.-H. Fu, *Biomaterials* **2009**, *30*, 4178.
[118] T. Matsumoto, M. Okazaki, M. Inoue, S. Yamaguchi, T. Kusunose, T. Toyonaga, Y. Hamada, J. Takahashi, *Biomaterials* **2004**, *25*, 3807.
[119] M. Kay, R. A. Young, A. S. Posner, *Nature* **1964**, *204*, 1050.
[120] X. Yan, C. Yu, X. Zhou, J. Tang, D. Zhao, *Angew. Chem. Int. Ed.* **2004**, *43*, 5980.
[121] W. Xia, J. Chang, *J. Controlled Release* **2006**, *110*, 522.
[122] T. A. Ostomel, Q. Shi, C. -K. Tsung, H. Liang, G. D. Stucky, *Small* **2006**, *2*, 1261.
[123] J. Ryu, S. H. Ku, H. Lee, C. B. Park, *Adv. Funct. Mater.* **2010**, *20*, 2132.
[124] S. H. Ku, J. Ryu, S. K. Hong, H. Lee, C. B. Park, *Biomaterials* **2010**, *31*, 2535.
[125] S. Kim, C. B. Park, *Langmuir* **2010**, *26*, 14730.
[126] S. Kim, C. B. Park, *Biomaterials* **2010**, *31*, 6628.
[127] V. Ball, D. D. Frari, M. Michel, M. J. Buehler, V. Toniazzo, M. K. Singh, J. Gracio, D. Ruch, *J. Bionanosci.* **2012**, *2*, 16.
[128] B. P. Lee, P. B. Messersmith, J. N. Israelachvili, J. H. Waite, *Annu. Rev. Mater. Res.* **2011**, *41*, 99.
[129] D. V. Volodkin, N. I. Larionova, G. B. Sukhorukov, *Biomacromolecules* **2004**, *5*, 1962.
[130] Q. Zhao, B. Li, *Nanomed. Nanotechnol. Biol. Med.* **2008**, *4*, 302.
[131] Y. Zhao, Y. Lu, Y. Hu, J.-P. Li, L. Dong, L.-N. Lin, S.-H. Yu, *Small* **2010**, *6*, 2436.
[132] M. A. Rauschmann, T. A. Wichelhaus, V. Stirnal, E. Dingeldein, L. Zichner, R. Schnettler, V. Alt, *Biomaterials* **2005**, *26*, 2677.
[133] P. N. Kumta, C. Sfeir, D.-H. Lee, D. Olton, D. Choi, *Acta Biomater.* **2005**, *1*, 65.
[134] Y. Mizushima, T. Ikoma, J. Tanaka, K. Hoshi, T. Ishihara, Y. Ogawa, A. Ueno, *J. Controlled Release* **2006**, *110*, 260.
[135] K. Tomoda, H. Ariizumi, T. Nakaji, K. Makino, *Colloids Surf., B* **2010**, *76*, 226.
[136] S. Tarafder, S. Banerjee, A. Bandyopadhyay, S. Bose, *Langmuir* **2010**, *26*, 16625.
[137] A. Schulz, B. M. Liebeck, D. John, A Heiss, T. Subkowski, A. Böker, *J. Mater. Chem.* **2011**, *21*, 9731.
[138] S. Leprêtre, F. Chai, J.-C. Hornez, G. Vermet, C. Neut, M. Descamps, H. F. Hildebrand, B. Martel, *Biomaterials* **2009**, *30*, 6086.
[139] M.-Y. Ma, Y.-J. Zhu, L. Li, S.-W. Cao, *J. Mater. Chem.* **2008**, *18*, 2722.
[140] C. Zhang, C. Li, S. Huang, Z. Hou, Z. Cheng, P. Yang, C. Peng, J. Lin, *Biomaterials* **2010**, *31*, 3374.
[141] P. Yang, P. Yang, X. Teng, J. Lin, L. Huang, *J. Mater. Chem.* **2011**, *21*, 5505.
[142] B. Palazzo, M. Iafisco, M. Laforgia, N. Margiotta, G. Natile, C. L. Bianchi, D. Walsh, S. Mann, N. Roveri, *Adv. Funct. Mater.* **2007**, *17*, 2180.
[143] M. Iafisco, B. Palazzo, M. Marchetti, N. Margiotta, R. Ostuni, G. Natile, M. Morpurgo, V. Gandin, C. Marzano, N. Roveri, *J. Mater. Chem.* **2009**, *19*, 8385.
[144] W. Wei, G.-H. Ma, G. Hu, D. Yu, T. Mcleish, Z.-G. Su, Z.-Y. Shen, *J. Am. Chem. Soc.* **2008**, *130*, 15808.
[145] J. Wang, J.-S. Chen, J.-Y. Zong, D. Zhao, F. Li, R.-X. Zhuo, S.-X. Cheng, *J. Phys. Chem. C* **2010**, *114*, 18940.
[146] Y. Zhao, L.-N. Lin, Y. Lu, S. F. Chen, L. Dong, S.-H. Yu, *Adv. Mater.* **2010**, *22*, 5255.
[147] Z.-Z. Li, L.-X. Wen, L. Shao, J.-F. Chen, *J. Controlled Release* **2004**, *98*, 245.
[148] J.-F. Chen, H. -M. Ding, J.-X. Wang, L. Shao, *Biomaterials* **2004**, *25*, 723.
[149] J. Zhou, W. Wu, D. Caruntu, M. H. Yu, A. Martin, J. F. Chen, C. J. O'Connor, W. L. Zhou, *J. Phys. Chem. C* **2007**, *111*, 17473.
[150] J. Wang, H. Ding, X. Tao, J. Chen, *Nanotechnology* **2007**, *18*, 245705,
[151] B. G. De Geest, R. E. Vandenbroucke, A. M. Guenther, G. B. Sukhorukov, W. E. Hennink, N. N. Sanders, J. Demeester, S. C. De Smedt, *Adv. Mater.* **2006**, *18*, 1005.
[152] Z. She, M. N. Antipina, J. Li, G. B. Sukhorukov, *Biomacromolecules* **2010**, *11*, 1241.
[153] M.-L. De Temmerman, J. Demeester, F. De Vos, S. C. De Smedt, *Biomacromolecules* **2011**, *12*, 1283.
[154] S. Anandhakumar, V. Nagaraja, A. M. Raichur, *Colloids Surf., B* **2010**, *78*, 266.
[155] C. Peng, Q. Zhao, C. Gao, *Colloids Surf. A* **2010**, *353*, 132.
[156] Y.-L. Xie, M.-J. Wang, S.-J. Yao, *Langmuir* **2009**, *25*, 8999.
[157] Z. Wang, L. Qian, X. Wang, H. Zhu, F. Yang, X. Yang, *Colloids Surf., A* **2009**, *332*, 164.